J|A|C|S
ARTICLES
Published on Web 02/22/2006

Mid-Infrared Spectroscopy of Protected Peptides in the Gas Phase: A Probe of the Backbone Conformation

Isabelle Compagnon,[†] Jos Oomens,[†] Gerard Meijer,[‡] and Gert von Helden*[,‡]

Contribution from the FOM Institute for Plasma Physics Rijnhuizen, Edisonbaan 14, NL-3439 MN Nieuwegein, The Netherlands, and the Fritz-Haber-Institut der Max-Planck-Gesellschaft, Faradayweg 4-6, D-14195 Berlin, Germany

Received August 15, 2005; E-mail: helden@fhi-berlin.mpg.de

Abstract: Infrared/UV hole-burning spectroscopy is performed on individual conformers of the protected dipeptide Z-Aib-Pro-NHMe. The extended IR range probed in this study allows one to elucidate both the H-bonding motif (5−7 μm) as well as the backbone structure (7−10 μm). Comparison with DFT calculations shows that the backbone is locally constrained to an α-conformation by Aib and to a γ-turn by Pro. The γ-turn motif observed here is intriguing since the condensed phase structure is known to be a β-turn. This is the first actual observation of such a discrepancy, and it emphasizes the subtle balance between intra- and intermolecular forces, which is responsible for the relative stability of the different secondary structure motifs.

1. Introduction

For more than two decades, protected peptides have been used as model systems to understand the formation of the secondary structures observed in proteins. In addition, they are used in the development of peptidomimetics, and a control over the secondary structure is important for tuning the pharmacological properties.[1] The investigation of short sequences allows accounting for the role of a specific amino acid in the competition between different forms, such as helices, β-sheets, and reverse turns. Popular methods used to determine the structure of a peptide include circular dichroism, X-ray crystallography, nuclear magnetic resonance, and infrared vibrational spectroscopy.[2]

When designing peptides or proteins, it is of advantage to introduce key amino acids or amino acid sequences that have strong propensities to induce desired secondary structural motifs.[3,4] Two amino acids that have especially high preferences for particular secondary structural motifs are α-aminoisobutyric acid (Aib) and proline (Pro). The rare amino acid Aib contains two methyl groups on the C_α position, which induces severe sterical constraints for the conformations it can accommodate. For that reason, Aib has a strong propensity to form helix forms, such as right- or left-handed α-helices as well as 3_{10}-helices.[5] It can therefore be used as a "β-sheet breaker" to disrupt β-sheet structures that play a role in so-called conformational diseases.[6,7] The amino acid proline, which possesses a pyrrolidine ring, is unique of its kind and is often found in proteins as part of γ-turns and β-turns.[2]

Although Aib is one of the rare amino acids, it is naturally occurring in antibiotic peptides of microbial origin. These so-called peptaibols can form voltage-gated transmembrane ion channels.[4,8] Of those, a large fraction contains the segment Aib−Pro, and that sequence is held responsible for a "hinge" function in those peptides.

Thus, numerous studies have addressed the structure of model peptides containing the amino acids Aib and Pro. It is found that a guest Aib−Pro sequence inserted in a longer segment can initiate a 3_{10}-helix in the form of a β-turn structure,[9] while repetitive sequences of Aib−Pro form α-helices, 3_{10}-helices, or β-bend ribbons (a subtype of 3_{10}-helix).[10−12]

One model system that has been investigated is Z-Aib-Pro-NHMe (Z = benzyloxycarbonyl). This molecule has been studied in the crystalline phase[13] as well as in solution,[14] and detailed structural parameters could be deduced. In those environments, it is found that Z-Aib-Pro-NHMe contains a β-turn of type III with a hydrogen bond that links the C═O near the Z-cap with the N−H at the NHMe (see Figure 1).

[†] FOM Institute for Plasma Physics.
[‡] Fritz-Haber-Institut.

(1) Loughlin, W. A.; Tyndall, J. D. A.; Glenn, M. P.; Fairlie, D. P. *Chem. Rev.* **2004**, *104*, 6085−6117.
(2) Vass, E.; Hollosi, M.; Besson, F.; Buchet, R. *Chem. Rev.* **2003**, *103*, 1917−1954.
(3) DeGrado, W. F. *Chem. Rev.* **2001**, *101*, 3025−3026.
(4) Venkataram Prasad, B. V.; Balaram, P. *CRC Crit. Rev. Biochem.* **1981**, *16*, 307−348.
(5) Toniolo, T.; Crisma, M.; Formaggio, F.; Peggion, C. *Biopolymers* **2001**, *60*, 397−419.
(6) Kumita, J. R.; Weston, C. J.; Choo-Smith, L.; Woolley, A. G.; Smart, O. S. *Biochemistry* **2003**, *42*, 4492−4498.
(7) Formaggio, F.; Bettio, A.; Moretto, V.; Crisma, M.; Toniolo, C.; Broxterman, Q. B. *J. Pept. Sci* **2003**, *9*, 461−466.
(8) Sansom, M. S. P. *Q. Rev. Biophys.* **1993**, *26*, 365−421.
(9) Karle, I. L.; Flippen-Anderson, J. L.; Uma, K.; Balaram, H.; Balaram, P. *Biopolymers* **1990**, *29*, 1433−1442.
(10) Aubry, A.; Bayeul, D.; Brückner, H.; Schiemann, N.; Benedetti, E. *J. Pept. Sci* **1998**, *4*, 502−510.
(11) Karle, I. L.; Flippen-Anderson, J.; Sukumar, M.; Balaram, P. *Proc. Natl. Acad. Sci. U.S.A.* **1987**, *84*, 5087−5091.
(12) Di Blasio, B.; Pavone, V.; Saviano, M.; Lombardi, A.; Nastri, F.; Pedone, C.; Benedetti, E.; Crisma, M.; Anzolin, M.; Toniolo, C. *J. Am. Chem. Soc.* **1992**, *114*, 6273−6278.
(13) Prasad, B. V.; Shamala, N.; Nagaraj, R.; Chandrasekaran, R.; Balaram, P. *Biopolymers* **1979**, *18*, 1635−1646.
(14) Rao, C. P.; Nagaraj, R.; Rao, C. N. R.; Balalram, P. *Biochemistry* **1980**, *19*, 425−431.

 10.1021/ja055378h CCC: $33.50

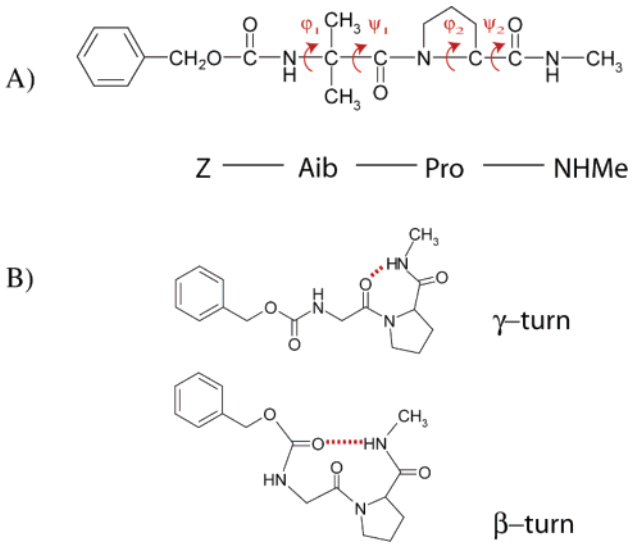

Figure 1. (A) Structure of Z-Aib-Pro-NHMe. The rare amino acid Aib is C-α-tetrasubstituted. This introduces conformational restrictions on the backbone of peptides containing this residue. The arrows indicate the dihedral Ramachandran angles. (B) The γ-turn and β-turn are the two remarkable H-bonded motifs that may be accommodated in this dipeptide.

An important question is in how far this is an intrinsic property of the molecule itself or whether the propensity to form such a structure is maybe also influenced by interactions of the molecule with its environment. In the condensed phase, a subtle balance between inseparable parameters, namely, the residue-specific effects and the interactions with the environment, governs the stability of these structures. In the gas phase, molecules can be studied in an environment where interacting molecules (solvent) are either completely absent or where they can be added one-by-one. In recent years, the development of spectroscopic methods coupled with (bio) molecular beam experiments, along with the increase of high-level quantum calculations, enabled the study of biological systems in the gas phase.

Already in the 80s, UV hole-burning techniques coupled to molecular beam methods have demonstrated that different conformers of simple amino acids can be selectively excited and investigated.[15] When coupled to a tunable infrared (IR) laser, hole-burning spectroscopy allows one to record conformer-specific IR spectra in a heterogeneous mixture of conformations.[16−18] Conformer selectivity is obtained through selective and resonant UV excitation of the peptide, and therefore, this method has long been restricted to peptides containing an aromatic amino acid (Phe, Tyr, or Trp). Recently, we have shown that, by including an aromatic UV chromophore in the protecting function, this method can be applied to any peptide.[19]

In the 3 μm IR spectral region, the N−H stretching motion allows for the unraveling of the hydrogen-bonding network in the molecules.[20−25] Alternatively, the Amide I and II modes (peptidic C═O stretch and N−H bend, respectively) can be probed between 5 and 7 μm. They too give detailed information on the hydrogen-bonding network, while lower frequency modes can then be used to assign the backbone and side chain conformations in greater detail. A complication in performing experiments at 5 μm and longer wavelengths is that it is more difficult to generate laser radiation in that range. Recently, tabletop systems[26] and free electron lasers[27] have been shown to be useful in that range for experiments on gas-phase biomolecules. Systems studied using those lasers include protected and unprotected amino acids[28−31] as well as small peptides.[19,32−37]

Here, we present results from infrared spectroscopic investigations of Z-Aib-Pro-NHMe in the spectral range of 5−10 μm using the Free Electron Laser for Infrared Experiments (FELIX).[27] The spectra obtained are compared to results from ab initio calculations, and it will be shown that the combination of experimental and theoretical IR spectra can yield detailed structural information.

2. Experimental Section

2.1. Peptide Synthesis. The synthesis of Z-Aib-Pro-NHMe is performed in solution. The capped amino acids Z-Aib and Z-Pro were purchased from Sigma-Aldrich. Z-Pro-NHMe is synthesized by adding methylamine to Z-Pro after activation with *N*-methylmorpholine and isobutylchloroformate. The Z-cap is removed by catalytic hydrogenation to yield Pro-NHMe. Then, Z-Aib is coupled to Pro-NHMe following the standard dicyclohexylcarbodiimide route to yield Z-Aib-Pro-NHMe.

2.2. Experimental Setup. The experimental setup consists of a pulsed molecular beam machine equipped with a laser desorption source coupled to a time-of-flight mass spectrometer (TOF).[19,30] The sample is mixed with graphite powder, rubbed onto a graphite bar, and placed directly under the nozzle of the pulsed valve, through which argon with a backing pressure of 3 bar is expanded as a buffer gas. The molecules are desorbed from the sample using a ~10 mJ pulse at 1064 nm, synchronized with the opening of the pulsed valve in order to achieve an efficient internal cooling in the supersonic expansion of the argon beam. The neutral molecular beam is skimmed and enters the extraction region of the TOF. The molecules are ionized with a tunable UV laser beam (frequency doubled output of a dye laser pumped

(15) Rizzo, T. R.; Park, Y. D.; Levy, D. H. *J. Chem. Phys.* **1986**, *85*, 6945−6951.
(16) Page, R. H.; Shen, Y.; Lee, Y. T. *J. Chem. Phys.* **1988**, *88*, 4621−4636.
(17) Zwier, T. S. *Annu. Rev. Phys. Chem.* **1996**, *47*, 205−241.
(18) Ebata, T.; Fujii, A.; Mikami, N. *Int. Rev. Phys. Chem.* **1998**, *17*, 331−361.
(19) Compagnon, I.; Oomens, J.; Bakker, J.; Meijer, G.; von Helden, G. *Phys. Chem. Chem. Phys.* **2005**, *7*, 13−15.
(20) Snoek, L. C.; Robertson, E. G.; Kroemer, R. T.; Simons, J. P. *Chem. Phys. Lett.* **2000**, *321*, 49−56.
(21) Snoek, L. C.; Kroemer, R. T.; Hockridge, J. P.; Simons, J. P. *Phys. Chem. Chem. Phys.* **2001**, *3*, 1819−1826.
(22) Dian, B. C.; Longarte, A.; Mercier, S.; Evans, D. A.; Wales, D. J.; Zwier, T. S. *J. Chem. Phys.* **2002**, *117*, 10688−10702.
(23) Hünig, I.; Kleinermanns, K. *Phys. Chem. Chem. Phys.* **2004**, *6*, 2650−2658.
(24) Chin, W.; Mons, M.; Dognon, J.-P.; Piuzzi, F.; Tardivel, B.; Dimicoli, I. *Phys. Chem. Chem. Phys.* **2004**, *6*, 2700−2709.
(25) Gerhards, M.; Unterberg, C. *Phys. Chem. Chem. Phys.* **2002**, *4*, 1760−1765.
(26) Gerhards, M. *Opt. Commun.* **2004**, *241*, 493−497.
(27) Oepts, D.; van der Meer, A. F. G.; Amersfoort, P. W. *Infrared Phys. Technol.* **1995**, *36*, 297−308.
(28) Gerhards, M.; Unterberg, C.; Gerlach, A.; Jansen, A. *Phys. Chem. Chem. Phys.* **2004**, *6*, 2682−2690.
(29) Gerhards, M.; Unterberg, C.; Gerlach, A. *Phys. Chem. Chem. Phys.* **2002**, *4*, 5563−5565.
(30) Bakker, J. M.; Mac Aleese, L.; Meijer, G.; von Helden, G. *Phys. Rev. Lett.* **2003**, *91*, 203003.
(31) Chin, W.; Mons, M.; Dognon, J.-P.; Mirasol, R.; Chass, G.; Dimicoli, I.; Piuzzi, F.; Butz, P.; Tardivel, B.; Compagnon, I.; von Helden, G.; Meijer, G. *J. Phys. Chem. A* **2005**, *109*, 5281−5288.
(32) Fricke, H.; Gerlach, A.; Unterberg, C.; Rzepecki, P.; Schrader, T.; Gerhards, M. *Phys. Chem. Chem. Phys.* **2004**, *6*, 4636−4641.
(33) Unterberg, C.; Gerlach, A.; Schrader, T.; Gerhards, M. *J. Chem. Phys.* **2003**, *118*, 8296−8300.
(34) Bakker, J. M.; Plützer, C.; Hünig, I.; Häber, T.; Compagnon, I.; von Helden, G.; Meijer, G.; Kleinermanns, K. *Chem. Phys. Chem.* **2005**, *6*, 120−128.
(35) Chin, W.; Compagnon, I.; Dognon, J.-P.; Canuel, C.; Piuzzi, F.; Dimicoli, I.; von Helden, G.; Meijer, G.; Mons, M. *J. Am. Chem. Soc.* **2005**, *127*, 1388−1389.
(36) Chin, W.; Dognon, J.-P.; Canuel, C.; Piuzzi, F.; Dimicoli, I.; Mons, M.; Compagnon, I.; von Helden, G.; Meijer, G. *J. Chem. Phys.* **2005**, *122*, 54317.
(37) Chin, W.; Dognon, J.-P.; Piuzzi, F.; Tarvidel, B.; Dimicoli, I.; Mons, M. *J. Am. Chem. Soc.* **2005**, *127*, 707−712.

with the third harmonic of a Nd:YAG laser) crossing the molecular beam perpendicularly. The ions are detected on a microchannel plate detector, and the TOF transient is recorded and averaged using a digital oscilloscope.

Vibrational spectroscopy is performed using the infrared radiation produced by the Free Electron Laser for Infrared Experiments (FELIX).[27] FELIX produces ~5 μs duration pulses over a wide tuning range (3−250 μm) at a bandwidth of about 0.5% of the central wavelength with a typical pulse energy of 60 mJ. The IR laser beam is aligned perpendicularly to the molecular beam and counter propagating to the UV beam.

Ionization of the Z-Aib-Pro-NHMe molecule is conveniently possible via a resonant two-photon process (R2PI) around 265 nm on the Z-chromophore built in the protecting function. To obtain the R2PI spectrum, the intensity of the ion signal on the mass channel corresponding to the parent peptide (347 amu) is monitored as a function of the UV excitation wavelength. This spectrum is a superposition of the R2PI spectra of all conformers present in the molecular beam.

The ionization laser is then parked on the S_1-S_0 transition of the conformer of interest, and the IR laser, which is fired just before the UV laser, is scanned over the fingerprint region of the peptide (900−1850 cm^{-1}). When the IR laser is resonant with an infrared transition of the molecule, the vibrational ground state of the S_0 state is depopulated, resulting in a dip of the ion signal. At each IR wavelength, the signal obtained when FELIX is irradiating the beam is divided by the signal obtained when FELIX is not on and the natural logarithm is taken. The FELIX fluence is not constant over the range scanned in this experiment, and the IR spectra are corrected for this. An IR absorption spectrum is recorded independently for each of the UV resonances in the R2PI spectrum. Different conformers usually have different IR spectra, and it is thus possible to assign the various bands in the R2PI spectrum to the different conformers present in the beam.

2.3. Calculations. The molecule contains many rotatable bonds, and the conformational space is therefore very large. In fact, the molecule is much too flexible so that a systematic search through all possible conformations is presently not feasible. The approach used here to find low energy conformations uses a combined empirical force-field−density functional method. An empirical force field is used in restrained and unrestrained molecular dynamics/simulated annealing calculations to locate local minima on the potential energy surface. Those structures are then further optimized using density functional theory, and a vibrational analysis is performed.

The force field calculations are performed using the general amber force field (GAFF)[38] as implemented in Amber8.[39] Atomic charges are calculated using a restrained electrostatic potential fit of a HF/6-31G-(d) charge distribution. Several hundred 100 ps long molecular dynamics/simulated annealing calculations were performed. During the run, the temperature is slowly reduced from 900 to 0 K. In some calculations, the geometry is constrained to include hydrogen bonds to force the molecule to γ- or β-turn structures as shown in Figure 1B. Those constraints are then slowly lifted as the molecule cools. The lowest energy structures are then investigated using density functional methods. Those calculations are performed using the B3LYP method, employing a 6-31+G(d) basis. Further, single point calculations using the B3LYP/6-31+G(d) structure at the MP2 level with a 6-311+G-(d,p) were performed.

The calculations lead to two families of stable structures, γ-turns and β-turns (see Figure 1). In the first case, the γ-turn is always located on the amino acid proline with the typical Ramachandran angles [$\varphi_2 = -83°$, $\psi_2 = +75°$], while Aib accommodates a remarkable helix or β-strand structure, or some intermediate conformation. Three common types of β-turns are obtained in the course of the calculations, namely, the type I, type II′, and type III. These types of turns are permitted, but their reverse forms (type I′, type II, and type III′) cannot occur because of the chiral restriction introduced by the proline ring. As often observed for biomolecules, the different minima lie in a close energy range (within 27 kJ/mol).

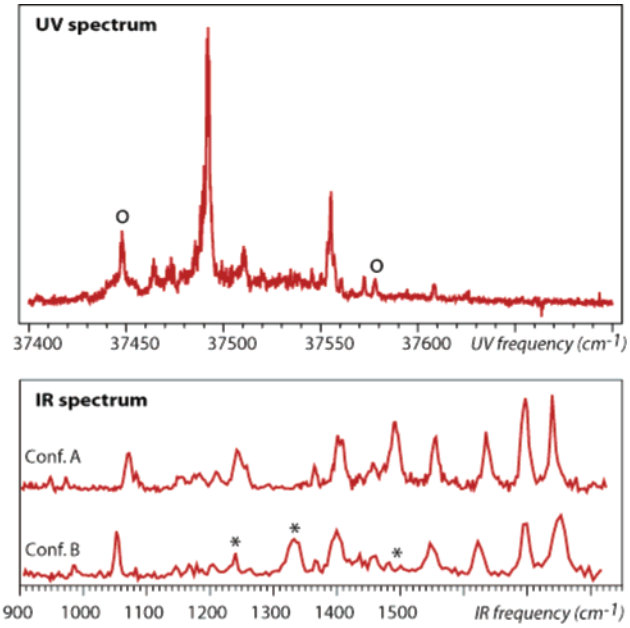

Figure 2. In the top part, the R2PI spectrum of Z-Aib-Pro-NHMe is shown. IR−UV hole-burning experiments allow one to identify the different conformers; conformer A is the most abundant with more than 90% of the ion signal. The two peaks marked with circles belong to conformer B. In the bottom part, the IR spectra of A and B are shown. Peaks in which the two spectra differ most are marked by stars.

3. Results

3.1. R2PI Spectrum and IR Diagnostic of the Conformers. The R2PI spectrum recorded in the range of 37 400−37 700 cm^{-1} is shown in the top trace of Figure 2. More than 15 peaks appear in the range from 37 440 to 37 610 cm^{-1}. Most of them are well resolved and background free, except for those arising on the red shoulder of the most intense feature at 37 492 cm^{-1}.

IR−UV hole-burning spectra are recorded for 15 UV wavelengths, covering the main peaks in the R2PI spectrum. When those IR−UV spectra are the same, one can assume that the corresponding molecules have the same conformation. It is observed that most of the vibrational spectra are identical and are attributed to a conformer that we label A; only the two peaks at 37 448 and 37 578 cm^{-1} (marked with circles in Figure 2) show a different IR signature and are attributed to a conformer that we label B. Judging from the intensities in the UV spectrum, the abundance of conformer A is more than 1 order of magnitude higher than the abundance of conformer B.

3.2. IR Spectra of Conformers A and B. The vibrational spectra of conformer A and conformer B are recorded with the ionization laser parked on the peaks at 37 492 and 37 448 cm^{-1}, respectively. The two spectra are presented in the lower part of Figure 2 and can be seen to be clearly different.

In both spectra, the three intense peaks on the blue side, between 1600 and 1800 cm^{-1}, can be assigned to the Amide I modes, resulting from the three C═O oscillators on the peptidic backbone. For both conformers A and B, their positions and relative intensities are rather similar, indicating a similar H-bonding motif.

In the spectrum of A, two peaks at 1490 and 1550 cm^{-1} can be assigned to the Amide II modes, resulting from the N−H

(38) Wang, J.; Wolf, R. M.; Caldwell, J. W.; Kollman, P. A.; Case, D. A. *J. Comput. Chem.* **2004**, *25*, 1157−1174.
(39) Case, D. A.; et al. *AMBER 8*; University of California, San Francisco, 2004.

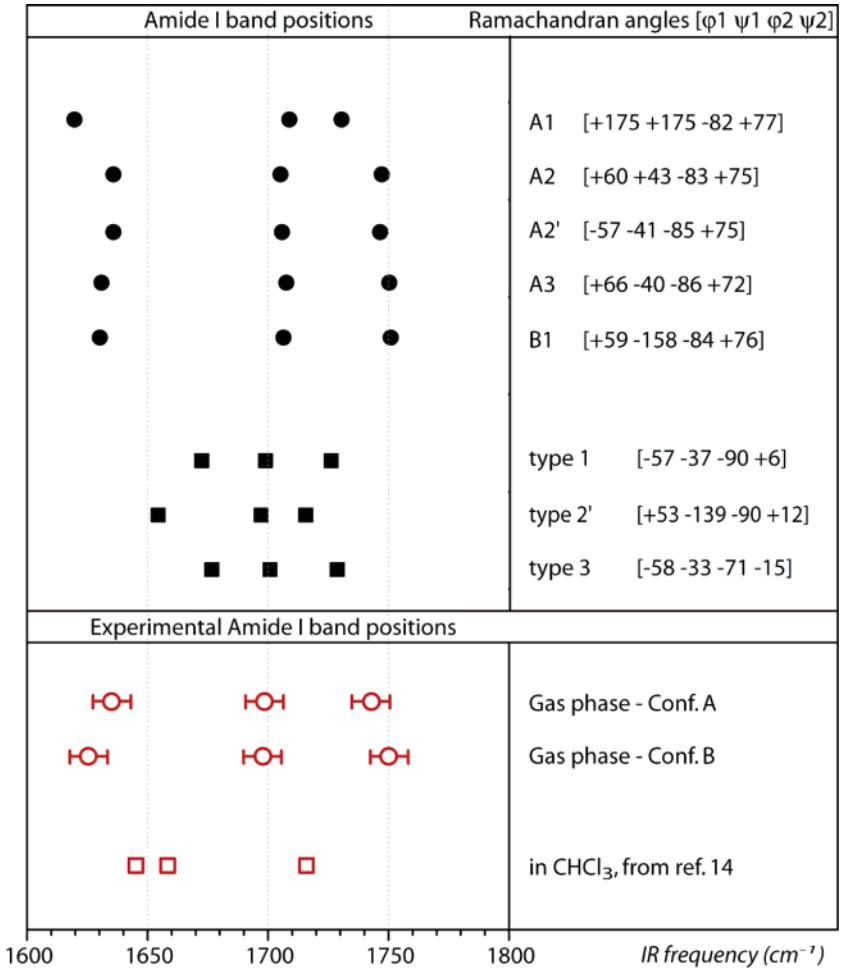

Figure 3. Upper panel: The position of the Amide I bands (scaled by 0.98) is shown for a selection of calculated structures. The γ-turns are plotted with closed circles and the β-turns with closed squares. Bottom panel: Experimental gas-phase position of the Amide I bands (this study, open circles) and in $CHCl_3$ (open squares).

bending motion of the two peptidic N−H groups. In the spectrum of B, the higher frequency one of the two is observed at essentially the same position. The lower frequency peak of the two, on the other hand, is apparently absent or at least severely shifted in position. This implies that something dramatic must have happened to one of the N−H groups in B. Below, we will see that this difference in the spectra is caused by the peptidic linkage at the Z-group being in an unusual cis-orientation. The most noticeable differences between the spectra of A and B are indicated with stars on the experimental spectrum of conformer B. Besides the mode at 1490 cm^{-1}, a mode at 1240 cm^{-1} is present for conformer A but absent or very weak for conformer B, and one mode at 1330 cm^{-1} is only observed for conformer B.

4. Discussion

The C═O stretching (Amide I) modes around 5 μm and the NH stretching modes around 3 μm are often used as diagnostics in IR spectroscopy of dissolved or solid peptides or proteins to identify their secondary structure. In many gas-phase experiments, these modes were shown to allow an accurate description of the intramolecular H-bonding network stabilizing the secondary structure along the peptide chain.

For both conformers investigated here, the three C═O stretching modes have a very similar Amide I signature. Their frequencies are [1739, 1697, 1635 cm^{-1}] and [1753, 1697, 1622 cm^{-1}], respectively, with an experimental bandwidth of 15 cm^{-1}. The absolute uncertainty in band position is estimated to be ± 8 cm^{-1}. The resemblance suggests that both conformers have the same H-bonding arrangement.

The experimental Amide I peak positions can be compared to theoretical predictions. In all calculated structures, the stretching mode of the C═O close to the Z-cap is observed most to the blue, the one of the center C═O linking the Aib with Pro most to the red, and the mode of the C═O close to the NHMe is observed between those two. In Figure 3, the experimental positions of the three C═O stretching modes of conformers A and B are compared with those of several calculated structures.

The calculated frequencies are scaled by a factor 0.98. Filled circles indicate γ-turns and filled squares β-turns; see Figure 1B for the hydrogen-bonding motif. Also given are the corresponding φ and ψ Ramachandran angles. In Table 1, the relative energies are given. As can be seen, DFT predicts γ-turn structure A1 and β-turn structure type I to be nearly isoenergetic.

The frequency of the C═O mode close to the NHMe group, between the two other peaks, is very similar for all structures considered. This is caused by the lack of involvement in H-bonding of this C═O group in all structures considered. In the β-turn structures, the C═O close to the Z is involved in

Table 1. Relative Energies (kJ/mol) of the Conformers Presented in Figure 3[a]

	B3LYP/6-31+G(d)	MP2/6-311+G(d,p)
A1	0.0[b] (0.2)	25.9 (27.0)
A2	1.5 (1.3)	9.9 (11.6)
A2′	3.4 (2.4)	16.2 (16.1)
A3	10.7 (11.6)	21.9 (23.7)
B1	19.0 (19.3)	18.9 (20.1)
type I	1.3 (0.0)	8.3 (7.9)
type II′	10.7 (11.0)	19.7 (20.9)
type III	1.2 (0.3)	0.0[c] (0.0)

[a] Shown in parentheses are the relative energies corrected for differences in zero-point energies using the B3LYP vibrational frequencies. The MP2 single point calculation is performed at the respective B3LYP geometry. [b] Total energy (hartree) = −1166.2240; the total zero-point energy for this conformer is 1109.3 kJ/mol. [c] Total energy (hartree) = −1163.2403.

H-bonding and shifts about 30 cm^{-1} to the red, compared to this group being free. Similarly, in the γ-turn structures, the oscillator most to the red (the central C═O) shifts by almost 50 cm^{-1} to the red upon being involved in a H-bond. Therefore, the Amide I motif of the γ-turns appears much wider than that of the β-turns. Comparison with the experimental frequencies (open squares) unambiguously shows that both conformers A and B are γ-turn structures and not β-turn structures.

The crystal structure of Z-Aib-Pro-NHMe has been determined directly by X-ray diffraction analysis by Prasad et al.[13] The set of angles [$\varphi_1 = -51°$, $\psi_1 = -39.7°$, $\varphi_2 = -65°$, $\psi_2 = -25.4°$] falls in the type III β-turn region of the conformational map, with a variation of no more than 10° from the "ideal" values [$\phi_1 = -60°$, $\psi_1 = -30°$, $\phi_2 = -60°$, $\psi_2 = -30°$].

Rao et al.[14] have recorded the infrared spectrum of this peptide in a solution of $CHCl_3$ in the Amide I region. The three C═O stretching modes were observed at 1715, 1658, and 1645 cm^{-1}. This motif was interpreted as a signature for the presence of a C_{10} H-bonded ring, which is compatible with the type III β-turn observed in the solid phase. To compare the solution-phase IR data with the present gas-phase measurements, the C═O stretching frequencies from ref 14 are shown in Figure 3 as well (open squares). It is noteworthy that the solvent induces a shift of the vibrational frequencies; therefore, the absolute values cannot be compared directly to our gas-phase measurements or calculations. Nevertheless, the overall Amide I motif in solution is rather compact, which indeed better matches with a β-turn structure (closed squares).

A comparison of the X-ray data[13] and solution IR data[14] with the results presented here leads to the conclusion that the secondary structure of the dipeptide Z-Aib-Pro-NHMe is different in the gas phase and in the condensed phase. This is a striking example of the delicate competition between two quasi-isoenergetic secondary structures; here the intrinsic preference is a γ-turn, but with the added interaction with other molecules, the β-turn is favored.

The Amide I calculations shown in Figure 3 cannot be used to tell which of the γ-turn structures are present in the experiment. To do this, the entire spectral range has to be

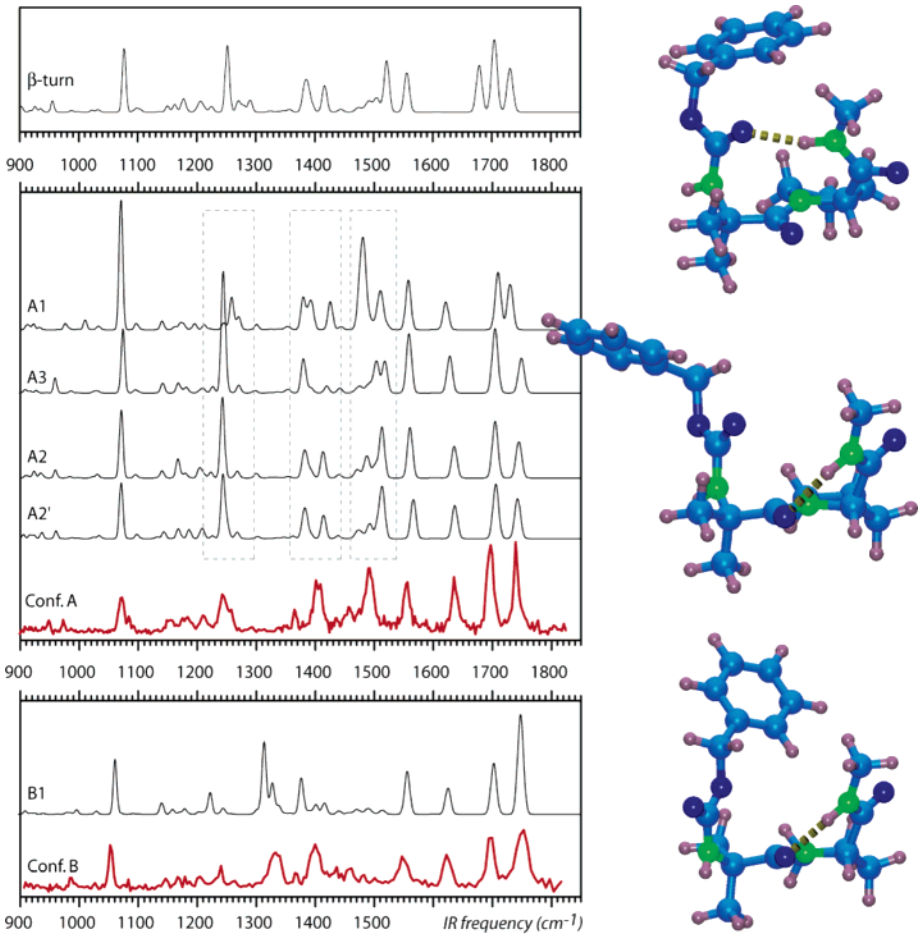

Figure 4. Vibrational spectra of conformers A and B (bold red line) compared to the calculated spectra of a variety of γ-turn structures (thin line). The structures shown are for the β-turn, A2′, and B1 conformer (top to bottom, respectively).

considered. The experimental spectrum of conformer A is compared to the calculated spectra of the four lowest energy γ-turns labeled A1, A2, A2′, and A3 in Figure 4.

The structures differ by the set of Ramachandran angles [φ_1, ψ_1] defining the orientation of the amino acid Aib. For each of them, different orientations of the Z-cap can occur: perpendicular pointing up, perpendicular pointing down, and in plane with respect to the plane of the first amide bond. This difference in Z-orientation does not significantly affect the energies or the IR spectra of the structures, and in the further discussion, we will ignore the orientation of this group. The conformation accommodated by the amino acid Aib is a β-sheet in A1, a helix in A2, an inverse helix in A2′, and an intermediate structure in A3. The peaks that are most diagnostic for a structure assignment are shown in Figure 4 in boxes. The structures A1 and A3 can be discarded by the comparison of their spectra in the mid-IR region of 1000−1600 cm^{-1} with the experimental spectra. Conformations A2 and A2′ show a good overall match with the experimental spectrum. These two conformations are very similar; they both are a helix followed with a γ-turn; however, A2 accommodates a right-handed helix, while A2′ accommodates the left-handed form. Their spectra mostly differ by the intensity of a weak feature at 1160 cm^{-1}.

The experimental spectrum of conformer B agrees very well with the calculated spectrum of a conformer labeled B1. In this structure, the Z-peptidic bond is in an unusual cis-configuration. This causes the corresponding N−H bending mode to shift to about 1400 cm^{-1}, couple strongly to other modes, and lose a large fraction of its oscillator strength. This cis-conformation is most likely an artifact caused by the linkage to the Z-cap which is, due to the presence of the second oxygen, different from a canonical peptidic bond.

It is at the moment unclear why a β-turn structure is observed in the condensed phase but is apparently not present in the gas-phase experiment. One has, of course, to be cautious to conclude from "we do not see it" that "it does not exist". One possibility is that the apparent absence of the β-turn structure is caused by a dramatic change of its UV excitation characteristics, compared to that of the γ-turn structure, and such effects have previously been observed to be of importance.[40] For example, the excitation energy to the S_1 state, its lifetime, or the ionization energy could be different between the two conformers to such an extent that, under the conditions employed, the β-turn structure is not detected, but that it is, however, nonetheless present in the beam.

The calculations indicate that β-turn structures are low energy structures. At the DFT level, three γ-turn and two β-turn structures are within 4 kJ/mol. MP2 calculations have previously been shown to give a good description of the conformational preferences of peptides.[37] When performing MP2 calculations for the systems presented here, the energetics change dramatically and, for example, the relative energy of the A1 conformer increases by 27 kJ/mol. The lowest energy conformer is now the type III β-turn structure with the first γ-turn structure being 12 kJ/mol higher in energy. There is, however, one possible pitfall in those calculations. At the DFT level, dispersive interactions are known to be not treated correctly. Those dispersive interactions are especially important for the interaction between the Z-cap and the rest of the molecule. When optimizing the geometry at the DFT level, we can therefore not expect that the orientation of the cap is correct. When doing then a single point MP2 calculation, a contribution due to dispersive interactions is suddenly present; however, the Z-cap might be accidentally oriented in either a favorable or unfavorable orientation. A possible solution would be to search the conformational space using MP2. This is, however, computationally very costly, and further, the important parameter here, the peptidic backbone, is known to be adequately described by DFT.

The clear observation that the γ-turn structure is present in the beam means that either the γ-turn structure is the lowest energy structure or the barrier separating the conformers is very high. In the latter case, the β-turn structure would be present in the beam, however, would not be detected due to some unknown experimental artifact. We find such a scenario less likely. A visual inspection of the structures indicates that a transition between β-turn and γ-turn does not involve a significant amount of atomic rearrangement or hydrogen bond breaking. It thus seems likely that the barrier for isomerization from a β-turn to a γ-turn structure is low.

The barrier to isomerize from cis to trans in a peptidic bond, on the other hand, is expected to be rather high. The initially warm molecules could thus find their way to the γ-turn minimum upon cooling; however, a fraction also gets trapped in a local minimum with the Z-cap peptidic bond in a cis-configuration.

5. Conclusions

In the dipeptide Z-Aib-Pro-NHMe presented here, the analysis of the Amide I motif successfully reveals that the proline forms a γ-turn. The amino acid Aib is not involved in the H-bonding, and β-turn structures that are observed in the condensed phase are not observed. The Amide I motif alone does not allow us to assign which of the various γ-turn structures is present in the experiment. Hence, additional information is required for a complete description of the secondary structure of the peptide. The mid-IR region (1000−1600 cm^{-1}) provides this supplementary diagnostic through a variety of "backbone modes" which are coupled over the whole backbone and are highly sensitive to its conformation.

Two conformers are observed in the molecular beam. In the main conformer, Aib accommodates a helix structure and Pro accommodates a γ-turn structure. Both amino acids maintain their individual preference in the dipeptide as if they would not interact, and no collective structure—such as the β-turn observed in the condensed phase—is formed in the gas phase. This example shows the importance of gas-phase investigations to disentangle the intrinsic properties of biomolecules from the role of their environment.

Acknowledgment. This work is part of the research program of FOM, which is financially supported by the Nederlandse Organisatie voor Wetenschappelijk Onderzoek (NWO). We gratefully acknowledge the skillful assistance by the FELIX staff.

Supporting Information Available: Complete ref 39 and Cartesian coordinates for the conformers presented in Figure 3 and Table 1. This material is available free of charge via the Internet at http://pubs.acs.org.

JA055378H

(40) Weinkauf, R.; Lehrer, F.; Schlag, E. W.; Metsala, A. *Faraday Discuss.* **2000**, *115*, 363−381.